J Biomol NMR (2011) 51:339–346
DOI 10.1007/s10858-011-9571-8

ARTICLE

# Multidimensional oriented solid-state NMR experiments enable the sequential assignment of uniformly $^{15}N$ labeled integral membrane proteins in magnetically aligned lipid bilayers

**Kaustubh R. Mote · T. Gopinath · Nathaniel J. Traaseth · Jason Kitchen · Peter L. Gor'kov · William W. Brey · Gianluigi Veglia**

Received: 23 June 2011 / Accepted: 11 August 2011 / Published online: 7 October 2011
© Springer Science+Business Media B.V. 2011

**Abstract** Oriented solid-state NMR is the most direct methodology to obtain the orientation of membrane proteins with respect to the lipid bilayer. The method consists of measuring $^{1}H$-$^{15}N$ dipolar couplings (DC) and $^{15}N$ anisotropic chemical shifts (CSA) for membrane proteins that are uniformly aligned with respect to the membrane bilayer. A significant advantage of this approach is that tilt and azimuthal (rotational) angles of the protein domains can be directly derived from analytical expression of DC and CSA values, or, alternatively, obtained by refining protein structures using these values as harmonic restraints in simulated annealing calculations. The Achilles' heel of this approach is the lack of suitable experiments for sequential assignment of the amide resonances. In this Article, we present a new pulse sequence that integrates proton driven spin diffusion (PDSD) with sensitivity-enhanced PISEMA in a 3D experiment ($[^{1}H,^{15}N]$-SE-PISEMA-PDSD). The incorporation of 2D $^{15}N/^{15}N$ spin diffusion experiments into this new 3D experiment leads to the complete and unambiguous assignment of the $^{15}N$ resonances. The feasibility of this approach is demonstrated for the membrane protein sarcolipin reconstituted in magnetically aligned lipid bicelles. Taken with low electric field probe technology, this approach will propel the determination of sequential assignment as well as structure and topology of larger integral membrane proteins in aligned lipid bilayers.

**Keywords** Oriented solid-state NMR (OSS-NMR) · Membrane proteins · Sequential assignment · Sarcolipin · Magnetically aligned bicelles · Proton driven spin diffusion · PISEMA · Sensitivity-enhancement

**Abbreviations**

| | |
|---|---|
| SLN | Sarcolipin |
| SERCA | sarcoplasmic reticulum $Ca^{2+}$-ATPase |
| DMPC | 1,2-dimyristoyl-sn-glycero-3-phosphocholine |
| D6PC | 1,2-dihexanoyl-sn-glycero-3-phosphocholine |
| POPC | 1-palmitoyl,2-oleyl-sn-glycero-3-phosphocholine |
| SE-PISEMA | Sensitivity enhanced polarization inversion spin exchange at magic angle |
| PISA | Polar index slant angle |

## Introduction

The complete determination of membrane protein structures requires the characterization of their architecture within the membrane (topology), which dictates their

**Electronic supplementary material** The online version of this article (doi:10.1007/s10858-011-9571-8) contains supplementary material, which is available to authorized users.

K. R. Mote · G. Veglia
Department of Chemistry, University of Minnesota, Minneapolis, MN 55455-0431, USA

T. Gopinath · N. J. Traaseth · G. Veglia (✉)
Department of Biochemistry, Molecular Biology and Biophysics, University of Minnesota, 207 Pleasant St. S. E, Minneapolis, MN 55455, USA
e-mail: vegli001@umn.edu

*Present Address:*
N. J. Traaseth
Chemistry Department, New York University, New York, NY 10003, USA

J. Kitchen · P. L. Gor'kov · W. W. Brey
National High Magnetic Field Laboratory, Tallahassee, FL 32310, USA

biological activity (White 2009). Oriented solid-state NMR (OSS-NMR) spectroscopy is uniquely suited to elucidate membrane protein topology (e.g., tilt and azimuthal or rotation angles) in both mechanically and magnetically aligned lipid bilayers (Ketchem et al. 1993; Valentine et al. 2001; Buck-Koehntop et al. 2005; De Angelis et al. 2006; Mani et al. 2006; Cady et al. 2009; Traaseth et al. 2009; Sharma et al. 2010; Verardi et al. 2011). To date, the majority of the solid-state NMR structures of isolated domains and intact membrane proteins deposited in the protein data bank originated from OSS-NMR or a combination of this approach with solution NMR restraints from micelle studies (i.e. hybrid approach) (http://www.drorlist.com/nmr/SPNMR.html).

In OSS-NMR, the membrane protein fingerprint is imaged by 2D separated local field (SLF) experiments (Hester et al. 1976). Pulse sequences such as PISEMA (Wu et al. 1994; Wang et al. 2000; Lee et al. 2004; Dvinskikh and Sandstrom 2005; Gopinath and Veglia 2009, 2010), SAMPI-4 (Nevzorov and Opella 2007; Gopinath et al. 2010), HIM-SELF (Yamamoto et al. 2006; Gopinath et al. 2010), and PELF (Soong et al. 2010) are routinely used to correlate backbone dipolar couplings (DC) with anisotropic chemical shifts (CSA) of uniformly $^{15}$N labeled proteins. These anisotropic parameters are used as orientation restraints for structure calculations, assuming prior knowledge of the CSA and DC tensors (Ketchem et al. 1993; Bertram et al. 2000; Shi et al. 2009b; Traaseth et al. 2009).

However, the bottleneck of the OSS-NMR remains the sequential assignment of the amide resonances. Currently, multiple selectively labeled samples in combination with periodic patterns of anisotropic NMR observables originating from regular secondary structures (Mesleh et al. 2002; Mascioni and Veglia 2003) are used to assign OSS-NMR spectra. In addition, several algorithms have been developed to obtain the resonance assignment through "shotgun" approaches (Marassi and Opella 2003) and geometric (Asbury et al. 2006) or exhaustive searches (Mascioni and Veglia 2003; Buffy et al. 2006b). Recently, Opella and co-workers (Lu et al. 2011) have suggested a new procedure for resonance assignment based on DC values measured in bicelles with orthogonal orientations (*flipped* and *unflipped*, where the orientation of the bilayer normal is parallel and perpendicular to the direction of $B_o$, respectively) in combination with isotropic chemical shifts obtained from experiments in micelles or isotropic bicelles. These approaches, however, are labor intensive and time consuming, and if the protein structural domains deviate significantly from ideality, they become prone to errors.

A classical experiment used to correlate $^{15}$N resonances is the proton driven spin diffusion (PDSD) (Szeverenyi et al. 1982; Suter and Ernst 1985). The 2D and 3D versions of this experiment have been used to assign $^{15}$N backbone atoms in small proteins aligned in mechanically oriented lipid bilayers (Cross et al. 1983; Marassi et al. 1999). However, the low sensitivity of these experiments limited their application to only a few selected cases.

In the past few years, there has been a significant effort to develop robust bicelle systems to increase the sensitivity and resolution of SLF spectra (Aussenac et al. 2005; De Angelis and Opella 2007; Park and Opella 2010). Bicelles allow for higher and more consistent levels of hydration over mechanically aligned lipid bilayers, have a higher tolerance to protein concentrations, and increase the filling factor in the NMR coil. These factors in combination with low electric field (low-*E*) static probes (Gor'kov et al. 2007) dramatically boost both sensitivity and resolution of OSS-NMR techniques. These technological advancements have led to the development and use of several diffusion schemes, including mis-matched Hartman–Hahn (MMHH) (Nevzorov 2008; Knox et al. 2010), radio-frequency driven spin diffusion (RFDSD) (Xu et al. 2008), and proton spin diffusion (PSD) (Xu et al. 2011) to assign SLF spectra. Nonetheless, most of these applications have been done with 2D spectra, with inadequate resolution for obtaining a complete sequential assignment.

Here, we show that the combination of PDSD with sensitivity enhanced methods (Gopinath et al. 2010) is able to resolve most of the inter-residue correlations in a small (3.7 kDa) single-pass membrane protein sarcolipin (Odermatt et al. 1998; Mascioni et al. 2002; Tupling et al. 2002; Buffy et al. 2006a, b; Bhupathy et al. 2007; Traaseth et al. 2008). Unlike the other methods, PDSD has the advantage of higher signal-to-noise per unit time, and more importantly, it transfers the majority of magnetization between $i$ and $i + 1$ spin systems (Traaseth et al. 2010), allowing the classical main-chain *walk* to connect all of the amide resonances in proteins. These results establish the feasibility of sequential assignment of backbone resonances for membrane proteins reconstituted in magnetically oriented systems.

## Materials and methods

Uniformly $^{15}$N-sarcolipin (SLN) was expressed in *E. coli* and purified as previously described (Buck et al. 2003; Veglia et al. 2010). Briefly, SLN was expressed as a fusion protein with maltose binding protein (MBP), and was purified by affinity chromatography on an amylose column followed by cleavage with tobacco etch virus protease. SLN was collected as a precipitate after dialysis and further purified to homogeneity by reversed-phase HPLC. Lyophilized SLN was dissolved in NMR sample buffer containing 6.7 mg D6PC, 20 mM HEPES, 30 mM $CaCl_2$ or 100 mM NaCl, and 0.02% $NaN_3$. This preparation was

then added to 31 mg of long chain lipid (DMPC or DMPC/POPC 4/1 w/w) suspended in $H_2O$ to give a final lipid concentration of 25% (w/v). Bicelles with a q-ratio (long-chain lipid/short-chain lipid) of ~3.2 and an approximate order parameter of 0.8 (as measured by the comparison of the long-chain $^{31}P$ chemical shift in these aligned bicelles with the $^{31}P$ resonance in mechanically aligned lipid bilayers) were formed after several freeze–thaw–vortex cycles. To prepare *flipped* bicelles (i.e., with the membrane normal parallel with the direction of the static field), $YbCl_3$ was added to give a final concentration of 5 mM. All NMR experiments were performed on a 700 MHz VNMRS spectrometer at a temperature of 38°C for DMPC-D6PC bicelles and 25°C for DMPC-POPC-D6PC bicelles, with a low-*E* bicelle probe built by the RF Team at the National High Magnetic Field Laboratory (NHMFL) in Florida (Gor'kov et al. 2007). Cross polarization times of 500 μs or 1,000 μs with $^1H$ RF field strengths corresponding to 62.5 and 50.0 kHz were used for flipped and unflipped bicelles, respectively. FSLG decoupling was obtained by ramping the phase of $^1H$ RF with effective field strength corresponding to 62.5 and 50.0 kHz for flipped and unflipped bicelles, respectively. A recycle delay of 4 s was used in all experiments. A mixing time of 3 s was used during the PDSD element. An acquisition time of 5 ms was used in the direct dimension with 62.5 and 50.0 kHz SPINAL decoupling (Fung et al. 2000) on the proton channel for flipped and unflipped bicelles, respectively. Parameters for evolution in the indirect evolution are reported in figure legends. Spectra were processed in NMRPipe (Delaglio et al. 1995) and analyzed using Sparky (T. D. Goddard and D. G. Kneller, SPARKY 3, University of California, San Francisco). All 2D FIDs were zero-filled to a final matrix size of 8,192 × 4,096 (direct × indirect dimensions). For the SE-PISEMA and PDSD experiments, indirect dimensions were processed using the Rance–Kay and States mode, respectively (Kay et al. 1992). For the 3D SE-PISEMA-PDSD, the $t_1$ and $t_2$ dimensions were processed in Rance-Kay and States mode, respectively. A Lorentz-to-Gaussian window function (50–150 Hz) was used before Fourier transformation of the FID.

## Results and discussion

The most basic 2D PDSD experiment used to establish dipolar correlations among the backbone $^{15}N$ chemical shifts is shown in Fig. 1a (Szeverenyi et al. 1982; Suter and Ernst 1985; Cross et al. 1983). This element has been combined with the PISEMA pulse sequence as shown in Fig. 1b (Marassi et al. 1999). The spectra resulting from this experiment display 2D correlations between $^{15}N$ anisotropic chemical shifts and $^1H$–$^{15}N$ dipolar couplings overlaid with spin diffusion cross-peaks between the $^{15}N$ resonances.

The initial resonance assignments were carried out with 2D experiments where SLN was reconstituted in flipped bicelle samples. These samples do not require fast uniaxial rotational diffusion of the protein and give narrow linewidths with good sensitivity and resolution. Figure 2 shows spectra obtained from 2D PDSD ($^{15}N/^{15}N$; pulse sequence in Fig. 1a and spectrum in Fig. 2a) and 2D PISEMA-PDSD ($^1H$–$^{15}N/^{15}N$; pulse sequence in Fig. 1b and spectrum in

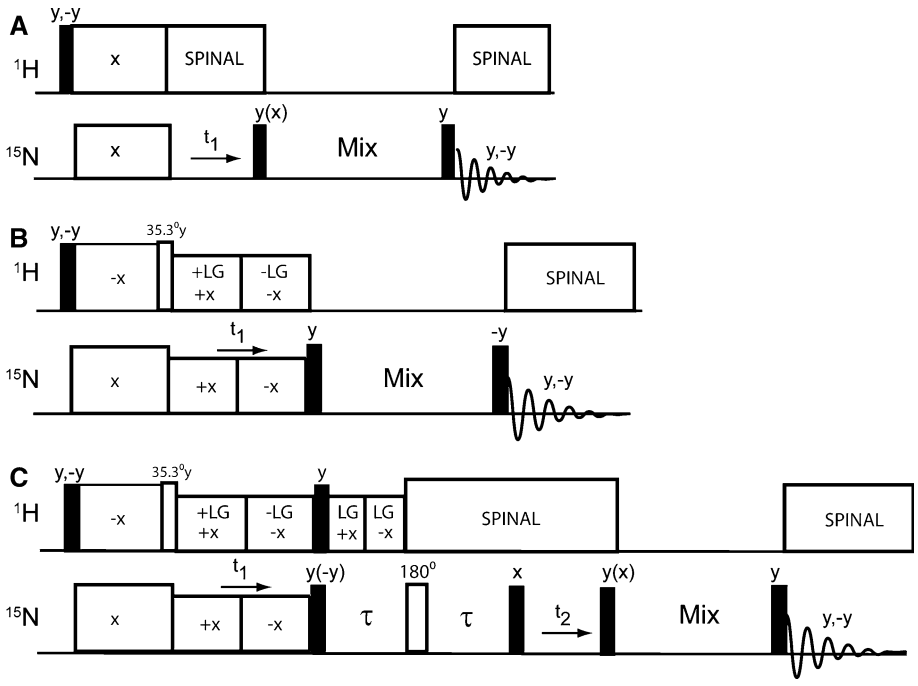


**Fig. 1** Pulse sequences used to assign SLN spectra. The PDSD was used for each mixing element in combination with **a** $^{15}N/^{15}N$ correlation, **b** $^1H$–$^{15}N/^{15}N$ correlation (2D-PISEMA-PDSD), and **c** $^1H$–$^{15}N/^{15}N/^{15}N$ (3D-[$^1H$,$^{15}N$]-SE-PISEMA-PDSD). A mixing time of 3 s was used for all experiments. The τ-value was set to 125 μ s for the 3D experiment in unflipped bicelles (Gopinath and Veglia 2009)

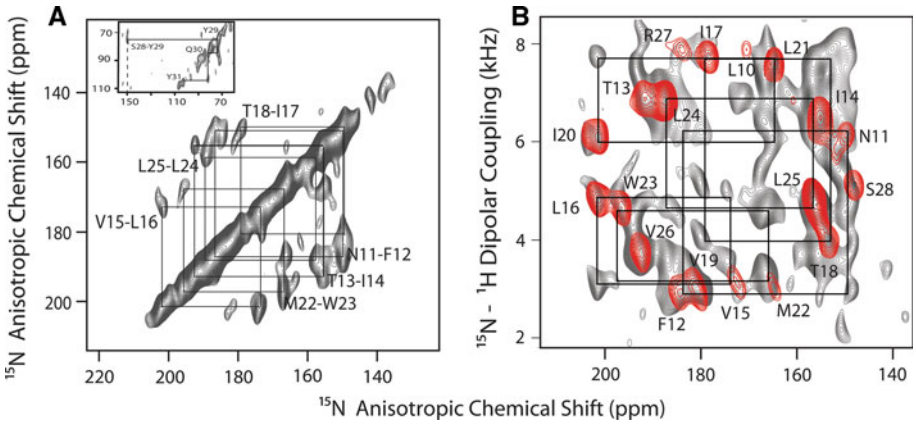


**Fig. 2** [U–$^{15}$N]-SLN spectra in flipped DMPC-D6PC bicelles at a protein to lipid ratio of 1:150 (~1.5 mg SLN) and temperature of 38°C. **a** $^{15}$N–$^{15}$N 2D correlation spectrum with a 3 s PDSD mixing time. 512 transients were co-added for 32 $t_1$ increments with a final $t_1$ evolution time of 1.5 ms. A few of the correlations obtained are shown in the figure. *Inset* Correlations between the transmembrane domain and the C-terminus. Cross peak intensities are ~20–30% of the diagonal peak intensity. **b** In red, [$^{1}$H,$^{15}$N]-SECT-PISEMA spectrum with 1,024 transients for each of the 21 $t_1$ increments and a constant time evolution period of 1.28 ms. In *grey* is the [$^{1}$H,$^{15}$N]-PISEMA-PDSD spectrum with 1,696 transients for each of the 20 $t_1$ increments. Only the transmembrane section of the spectrum is shown

Fig. 2b) correlation experiments in flipped DMPC-D6PC bicelles. These spectra were assigned by comparing with the SECT-PISEMA spectrum (Gopinath and Veglia 2010), which gave a significant increase in resolution due to 5–15% narrower linewidths, as compared to SE-PISEMA, in the dipolar dimension. The overlap of resonances in the 2D-PISEMA-PDSD makes it challenging to assign the cross-peaks. Although we were able to assign a total of 26 residues, there were many overlapped resonances and ambiguous assignments.

To resolve these ambiguities, we designed a new 3D experiment that combines the PISEMA-PDSD scheme with the sensitivity-enhancement (SE) element (Gopinath and Veglia 2009). The SE scheme detects both sine and cosine modulated dipolar coherences to boost the sensitivity of OSS-NMR spectra and can be used for both SLF and HETCOR experiments (Gopinath and Veglia 2010). In the 3D [$^{1}$H,$^{15}$N]-SE-PISEMA-PDSD experiment (pulse sequence in Fig. 1c and spectrum in Fig. 3), the magnetization is created via cross polarization and tilted at the magic angle. The $^{1}$H–$^{15}$N DC is evolved in the first indirectly detected dimension ($t_1$) in the same way as the PISEMA experiment using phase-modulated Lee-Goldburg homonuclear decoupling (Vinogradov et al. 1999). Subsequently, the *in-phase* single-quantum $^{15}$N magnetization is stored along the Z-axis, while the multiple-quantum magnetization is converted to single-quantum during the echo period ($2\tau$). Note that the optimal transfer during the echo period must be optimized for the average DC values within the sample. In the case of unflipped bicelle samples, the optimal delay was set to 3.0 kHz, while for flipped bicelle samples a value of 5.5 kHz was chosen. A 90° pulse is then applied which places magnetization in the XY plane to evolve in $t_2$ under $^{15}$N chemical shift. Following $t_2$ evolution, the coherences are positioned along the z-axis for the PDSD to take place, and finally tilted in the XY plane for detection during $t_3$. As a result this experiment correlates $^{1}$H–$^{15}$N dipolar coupling ($t_1$), $^{15}$N chemical shift ($t_2$), and $^{15}$N chemical shift ($t_3$), with dipolar cross-peaks that can be easily observed in the $^{15}$N/$^{15}$N dimensions. Figure 3 shows the strip plots from the 3D [$^{1}$H,$^{15}$N]-SE-PISEMA-PDSD spectrum in unflipped DMPC-POPC-D6PC bicelles. In this experiment, we set the PDSD mixing time to 3 s, which gives most intense cross-peaks per unit time in model compounds (Traaseth et al. 2010).

The intensities of the dipolar cross peaks with a 3 s PDSD mixing period were 20–30% of the diagonal peak intensities. Each diagonal peak displayed one or two intense correlations, corresponding to the adjacent residues in the primary sequence. Interestingly, a closer inspection revealed weaker $\{i, i + 2\}$ and $\{i, i + 3\}$ cross-peaks for some of the residues, showing that a residual long-range transfer can be observed in the PDSD experiment. Nonetheless, the most intense $\{i, i + 1\}$ correlations led to a straightforward determination of the backbone connectivity. In addition, we also observed that the cross-peak pattern obtained in flipped and unflipped bicelles is asymmetric with respect to the diagonal peaks as previously reported in the literature (Suter and Ernst 1985; Fu and Cross 1999; Knox et al. 2010). The stronger of the equivalent cross peaks was used for obtaining the assignments.

In total, correlations were obtained for 21 resonances from the datasets in flipped and unflipped bicelles. Figure 4 shows a comparison of SE-PISEMA spectra in flipped and unflipped bicelles. The assignments obtained for these spectra were confirmed by comparing the $^{15}$N–$^{1}$H DC for each residue. The order parameter for flipped bicelles relative to the unflipped bicelles was found to be ~0.94. The

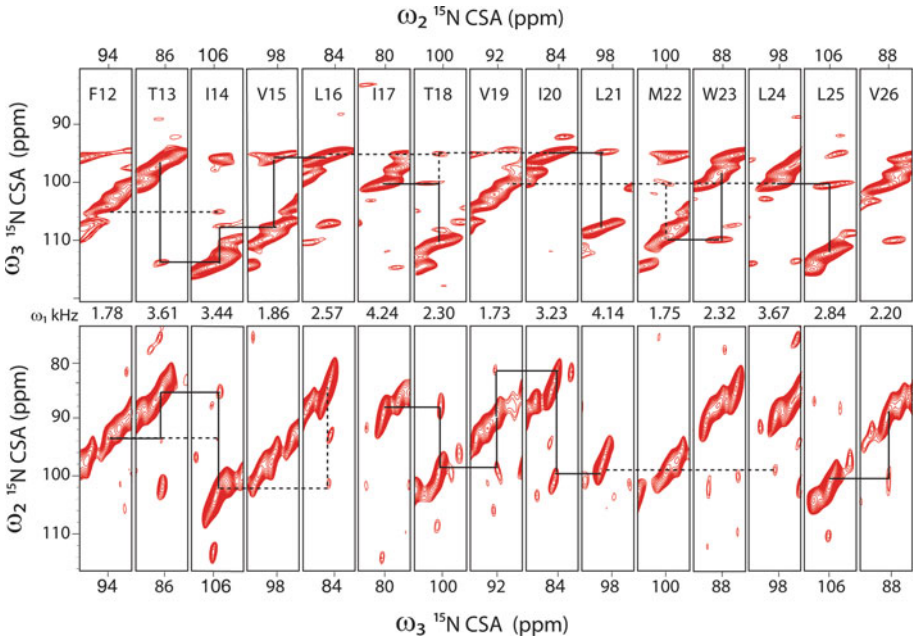


**Fig. 3** 3D strip plots at specific dipolar coupling values from a [$^1$H,$^{15}$N] SE-PISEMA-PDSD spectrum of [U–$^{15}$N]-SLN in unflipped DMPC-POPC-D6PC bicelles at 25°C and with a protein to lipid ratio of 1:75 (~3.0 mg SLN). A total of 40 transients were co-added for 20 $t_1$ and 32 $t_2$ increments corresponding to final $t_1$ and $t_2$ acquisition times of 2.4 ms and 1.5 ms, respectively. *Bold lines* indicate $\{i, i+1\}$ cross peaks and *dotted lines* indicate $\{i, i+2\}$ cross peaks. The same data set is plotted twice after interchanging the *X*- and *Y*-axes in order to account for the unequal intensities of the equivalent cross peaks in the spectrum. See Fig. S1 for representative 2D planes from this spectrum

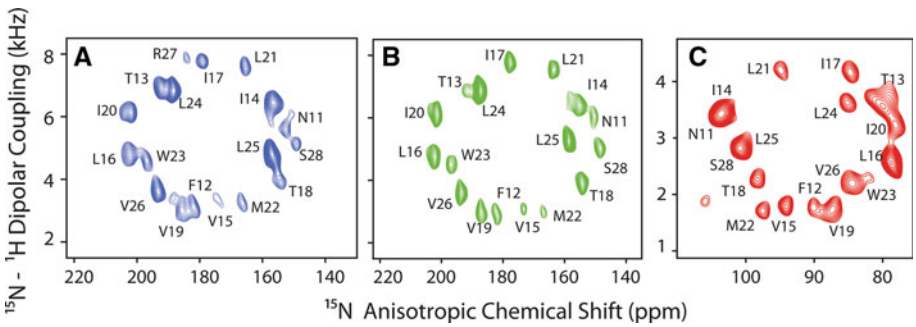


**Fig. 4** Comparison of independently obtained assignments for [U–$^{15}$N]-SLN in flipped and unflipped bicelles **a** [$^1$H,$^{15}$N] SE-PISEMA in flipped DMPC-D6PC bicelles with 256 transients and 25 $t_1$ increments at 38°C. **b** [$^1$H,$^{15}$N]-SE-PISEMA in flipped DMPC-POPC-D6PC bicelles with 256 transients and 25 $t_1$ increments at 25°C. **c** [$^1$H,$^{15}$N] SE-PISEMA in unflipped DMPC-POPC-D6PC bicelles with 288 transients and 25 $t_1$ increments with a final $t_1$ evolution time of 3.0 ms at 25°C. The $\tau$-value in sensitivity enhanced pulse sequence was set to 75 μs and 125 μs for flipped and unflipped bicelles, respectively

first assignment was made from the flipped spectrum by a cross-peak between residues 30 and 31 at the C-terminal end (Fig. 2a-inset). Another correlation between residue 29 at the C-terminus to residue 28 within the PISA wheel (Fig. 2a-inset) was observed in the spectra. Starting from these connectivities and using the spectra shown in Figs. 2 and 3, we unambiguously assigned 21 residues (N11–Y31) in agreement with the known α-helical structure of sarcolipin (Fig. 5; Table S1). The unflipped PDSD spectrum, however, did not show cross-peaks for C-terminal residues or for residues 16–17, possibly due to scaling of $^{15}$N–$^{15}$N DCs that reduces the probability for spin diffusion between $^{15}$N nuclei. In addition, cross peaks were indistinguishable for two residue pairs (21–22 and 23–24) that had nearly identical $^{15}$N CSA in the unflipped spectrum. Residues 6–10 were assigned based on the α-helical model in the flipped spectrum due to significant overlap in the unflipped PISEMA spectrum. Thus, we report assignments for 26 out of the 31 residues (R6–Y31) that were also consistent with selectively labeled PISEMA spectra obtained in mechanically aligned bilayers (Buffy et al. 2006b). Residues 1–5 form the dynamic N-terminus of the protein (Mascioni

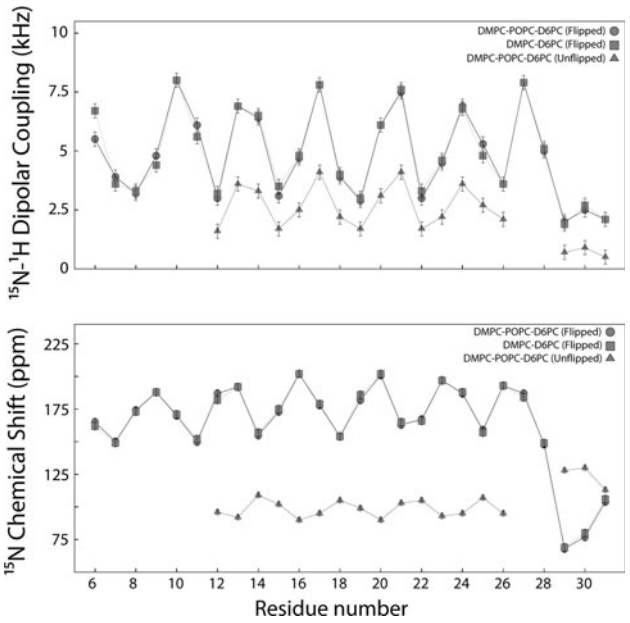


**Fig. 5** $^{15}$N CSA and $^{1}$H–$^{15}$N DC oscillation patterns for the assigned resonances of SLN in flipped and unflipped bicelles. The *error bars* reflect the average experimental linewidths

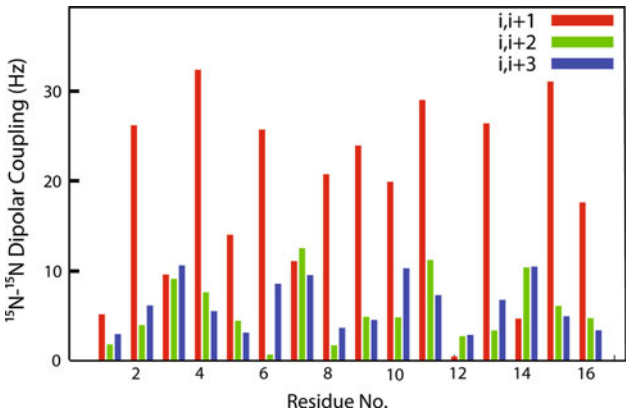


**Fig. 6** Calculated $^{15}$N–$^{15}$N dipolar couplings (absolute value) for an ideal $\alpha$-helix ($\phi = -60°$, $\psi = -45°$) tilted at an angle of 25° with respect to the membrane normal in flipped bicelles. DCs would be scaled by 0.5 in unflipped bicelles. Since the rate of PDSD is proportional to $\omega^2$ (Suter and Ernst 1985), it is expected that $^{15}$N nuclei with the largest DCs will be observed (i.e., primarily $\{i, i+1\}$ correlations). However, some of the $\{i, i+1\}$ DCs are close to zero and weaker correlations would be expected in the spectra

et al. 2002; Buffy et al. 2006a; Shi et al. 2009a), and could not be detected by cross-polarization used in our experiments.

The PISA wheel patterns in binary and ternary lipid bicelles are very similar. The resonances of the transmembrane domain were only slightly perturbed by these lipids, showing that the tilt and rotation angles are independent of these small changes in lipid composition and bilayer thickness. This allows for the possibility of screening different lipids to obtain optimal resolution without substantially affecting the topology and structure. Bicelles containing POPC improve sample stability by aligning at a lower temperature (25°C) compared to DMPC-only bicelles (38°C) and also increase bilayer thickness to better mimic the lipids present in the sarcoplasmic reticulum (primarily DOPC/DOPE). The DC and CSA oscillation pattern for the transmembrane domain of SLN is shown in Fig. 5. The regularity of the pattern and the uniformity of the PISA wheel suggest that the SLN transmembrane domain adopts a conformation close to an ideal $\alpha$-helix in lipid bilayers (Page et al. 2008).

The PDSD experiment depends on the $^{15}$N–$^{15}$N dipolar couplings (Fermi's golden rule) (Suter and Ernst 1985). Since the dipolar couplings have a periodic oscillation for helical proteins (Mesleh et al. 2002; Mascioni and Veglia 2003), this can lead to unequal cross peak intensities. In the most extreme cases, no cross peak can be observed if the DC value between $^{15}$N spins is equal to zero (Fig. 6). This effect is exacerbated by the unequal peak intensities obtained for SLF experiments, which has been shown to be a reflection of the mosaic spread of tilt angles (Buffy et al. 2006b; Quine et al. 2006). As a result, the cross-peak intensity cannot reliably be correlated to distance and should be used for assignment purposes only. The dependence of the cross-peak intensity on dipolar coupling (and hence distance) results in few cross peaks, most of which connect neighboring residues. The comparatively high intensity of the cross-peak is a direct result of using PDSD, which relies on $T_1$ rather than $T_{1\rho}$ spin exchange (Traaseth et al. 2010). Although there is evidence of $\{i, i+2\}$ and $\{i, i+3\}$ cross-peaks, these are without exception less intense than $\{i, i+1\}$ cross peaks and in practice, serve as an additional support for the assignment.

## Conclusions

We have obtained a de novo sequential assignment of the integral membrane protein SLN in magnetically aligned bicelles using only uniformly $^{15}$N labeled protein. This strategy is universally applicable to assigning membrane proteins with ideal and non-ideal $\alpha$-helical domains as well as $\beta$-barrels, since it does not assume ideal secondary structures. The use of proton driven spin diffusion facilitates semi-selective transfer of magnetization over short distances, which avoids ambiguity in resonance assignment. A robust assignment was made possible by a new 3D experiment that combined the sensitivity enhancement scheme with PISEMA and PDSD (3D-[$^{1}$H, $^{15}$N]-SE-PISEMA-PDSD). Further developments in sample preparation, pulse sequences, and innovative probe designs will

continue to advance this growing and exciting field. Although selective labeling and computational approaches will continue to be important, sequential assignment is the only approach that will be possible to fully assign large membrane proteins.

**Acknowledgments** The authors would like to thank Kim Ha and Raffaello Verardi for helping with protein purification and sample preparation. This work was supported by NIH to G.V. (GM 64742).

## References

Asbury T, Quine JR, Achuthan S, Hu J, Chapman MS, Cross TA, Bertram R (2006) PIPATH: an optimized algorithm for generating alpha-helical structures from PISEMA data. J Magn Reson 183:87–95

Aussenac F, Lavigne B, Dufourc EJ (2005) Toward bicelle stability with ether-linked phospholipids: temperature, composition, and hydration diagrams by H-2 and P-31 solid-state NMR. Langmuir 21:7129–7135

Bertram R, Quine JR, Chapman MS, Cross TA (2000) Atomic refinement using orientational restraints from solid-state NMR. J Magn Reson 147:9–16

Bhupathy P, Babu GJ, Periasamy M (2007) Sarcolipin and phospholamban as regulators of cardiac sarcoplasmic reticulum $Ca^{2+}$ ATPase. J Mol Cell Cardiol 42:903–911

Buck BA, Zamoon J, Kirby TL, DeSilva TM, Karim C, Thomas D, Veglia G et al (2003) Overexpression, purification, and characterization of recombinant ca-ATPase regulators for high-resolution solution and solid-state NMR studies. Protein Expr Purif 30:253–261

Buck-Koehntop BA, Mascioni A, Buffy JJ, Veglia G (2005) Structure, dynamics, and membrane topology of stannin: a mediator of neuronal cell apoptosis induced by trimethyltin chloride. J Mol Biol 354:652–665

Buffy JJ, Buck-Koehntop BA, Porcelli F, Traaseth NJ, Thomas DD, Veglia G (2006a) Defining the intramembrane binding mechanism of sarcolipin to calcium ATPase using solution NMR spectroscopy. J Mol Biol 358:420–429

Buffy JJ, Traaseth NJ, Mascioni A, Gor'kov PL, Chekmenev EY, Brey WW, Veglia G (2006b) Two-dimensional solid-state NMR reveals two topologies of sarcolipin in oriented lipid bilayers. Biochemistry 45:10939–10946

Cady SD, Mishanina TV, Hong M (2009) Structure of amantadine-bound M2 transmembrane peptide of influenza A in lipid bilayers from magic-angle-spinning solid-state NMR: the role of Ser31 in amantadine binding. J Mol Biol 385:1127–1141

Cross TA, Frey MH, Opella SJ (1983) Nitrogen-15 spin exchange in a protein. J Am Chem Soc 105:7471–7473

De Angelis AA, Opella SJ (2007) Bicelle samples for solid-state NMR of membrane proteins. Nat Protoc 2:2332–2338

De Angelis AA, Howell SC, Nevzorov AA, Opella SJ (2006) Structure determination of a membrane protein with two transmembrane helices in aligned phospholipid bicelles by solid-state NMR spectroscopy. J Am Chem Soc 128:12256–12267

Delaglio F, Grzesiek S, Vuister GW, Zhu G, Pfeifer J, Bax A (1995) NMRPipe: a multidimensional spectral processing system based on UNIX pipes. J Biomol NMR 6:277–293

Dvinskikh SV, Sandstrom D (2005) Frequency offset refocused PISEMA-type sequences. J Magn Reson 175:163–169

Fu R, Cross TA (1999) Solid-state nuclear magnetic resonance investigation of protein and polypeptide structure. Annu Rev Biophys Biomol Struct 28:235–268

Fung BM, Khitrin AK, Ermolaev K (2000) An improved broadband decoupling sequence for liquid crystals and solids. J Mag Res 142:97–101

Gopinath T, Veglia G (2009) Sensitivity enhancement in static solid-state NMR experiments via single- and multiple-quantum dipolar coherences. J Am Chem Soc 131:5754–5756

Gopinath T, Veglia G (2010) Improved resolution in dipolar NMR spectra using constant time evolution PISEMA experiment. Chem Phys Lett 494:104–110

Gopinath T, Verardi R, Traaseth NJ, Veglia G (2010) Sensitivity enhancement of separated local field experiments: application to membrane proteins. J Phys Chem B 114:5089–5095

Gor'kov PL, Chekmenev EY, Li C, Cotten M, Buffy JJ, Traaseth NJ, Veglia G, Brey WW (2007) Using low-E resonators to reduce RF heating in biological samples for static solid-state NMR up to 900 MHz. J Magn Reson 185:77–93

Hester RK, Ackerman JL, Neff BL, Waugh JS (1976) Separated local field spectra in NMR: determination of structure of solids. Phys Rev Lett 36:1081–1083

Kay L, Keifer P, Saarinen T (1992) Pure absorption gradient enhanced heteronuclear single quantum correlation spectroscopy with improved sensitivity. J Am Chem Soc 114:10663–10665

Ketchem RR, Hu W, Cross TA (1993) High-resolution conformation of gramicidin A in a lipid bilayer by solid-state NMR. Science 261:1457–1460

Knox RW, Lu GJ, Opella SJ, Nevzorov AA (2010) A resonance assignment method for oriented-sample solid-state NMR of proteins. J Am Chem Soc 132:8255–8257

Lee DK, Narasimhaswamy T, Ramamoorthy A (2004) PITANSEMA, a low-power PISEMA solid-state NMR experiment. Chem Phys Lett 399:359–362

Lu GJ, Son WS, Opella SJ (2011) A general assignment method for oriented sample (OS) solid-state NMR of proteins based on the correlation of resonances through heteronuclear dipolar couplings in samples aligned parallel and perpendicular to the magnetic field. J Magn Reson 209:195–206

Mani R, Cady SD, Tang M, Waring AJ, Lehrer RI, Hong M (2006) Membrane-dependent oligomeric structure and pore formation of a beta-hairpin antimicrobial peptide in lipid bilayers from solid-state NMR. Proc Natl Acad Sci USA 103: 16242–16247

Marassi FM, Opella SJ (2003) Simultaneous assignment and structure determination of a membrane protein from NMR orientational restraints. Protein Sci 12:403–411

Marassi FM, Gesell JJ, Valente AP, Kim Y, Oblatt-Montal M, Montal M, Opella SJ (1999) Dilute spin-exchange assignment of solid-state NMR spectra of oriented proteins: acetylcholine M2 in bilayers. J Biomol NMR 14:141–148

Mascioni A, Veglia G (2003) Theorotical analysis of residual dipolar couplings in regular secondary structure of proteins. J Am Chem Soc 125:12520–12526

Mascioni A, Karim C, Barany G, Thomas DD, Veglia G (2002) Structure and orientation of sarcolipin in lipid environments. Biochemistry 41:475–482

Mesleh MF, Veglia G, DeSilva TM, Marassi FM, Opella SJ (2002) Dipolar waves as NMR maps of protein structure. J Am Chem Soc 124:4206–4207

Nevzorov AA (2008) Mismatched hartmann-hahn conditions cause proton-mediated intermolecular magnetization transfer between dilute low-spin nuclei in NMR of static solids. J Am Chem Soc 130:11282–11283

Nevzorov AA, Opella SJ (2007) Selective averaging for high-resolution solid-state NMR spectroscopy of aligned samples. J Magn Reson 185:59–70

Odermatt A, Becker S, Khanna VK, Kurzydlowski K, Leisner E, Pette D, MacLennan DH (1998) Sarcolipin regulates the activity of

SERCA1, the fast-twitch skeletal muscle sarcoplasmic reticulum $Ca^{2+}$ -ATPase. J Biol Chem 273:12360–12369

Page RC, Kim S, Cross TA (2008) Transmembrane helix uniformity examined by spectral mapping of torsion angles. Structure 16:787–797

Park SH, Opella SJ (2010) Triton X-100 as the "short-chain lipid" improves the magnetic alignment and stability of membrane proteins in phosphatidylcholine bilayers for oriented-sample solid-state NMR spectroscopy. J Am Chem Soc 132: 12552–12553

Quine JR, Achuthan S, Asbury T, Bertram R, Chapman MS, Hu J, Cross TA (2006) Intensity and mosaic spread analysis from PISEMA tensors in solid-state NMR. J Magn Reson 179: 190–198

Sharma M, Yi M, Dong H, Qin H, Peterson E, Busath DD, Zhou HX, Cross TA (2010) Insight into the mechanism of the influenza A proton channel from a structure in a lipid bilayer. Science 330: 509–512

Shi L, Cembran A, Gao J, Veglia G (2009a) Tilt and azimuthal angles of a transmembrane peptide: a comparison between molecular dynamics calculations and solid-state NMR data of sarcolipin in lipid membranes. Biophys J 96:3648–3662

Shi L, Traaseth NJ, Verardi R, Cembran A, Gao J, Veglia G (2009b) A refinement protocol to determine structure, topology, and depth of insertion of membrane proteins using hybrid solution and solid-state NMR restraints. J Biomol NMR 44:195–205

Soong R, Smith PE, Xu J, Yamamoto K, Im SC, Waskell L, Ramamoorthy A (2010) Proton-evolved local-field solid-state NMR studies of cytochrome b5 embedded in bicelles, revealing both structural and dynamical information. J Am Chem Soc 132:5779–5788

Suter D, Ernst RR (1985) Spin diffusion in resolved solid-state NMR spectra. Phys Rev B Condens Matter 32:5608–5627

Szeverenyi NM, Sullivan MJ, Maciel GE (1982) Observation of spin exchange by two-dimensional fourier transform 13C cross polarization-magic-angle spinning (1969). J Mag Res 47: 462–475

Traaseth NJ, Ha KN, Verardi R, Shi L, Buffy JJ, Masterson LR, Veglia G (2008) Structural and dynamic basis of phospholamban and sarcolipin inhibition of Ca(2+)-ATPase. Biochemistry 47: 3–13

Traaseth NJ, Shi L, Verardi R, Mullen DG, Barany G, Veglia G (2009) Structure and topology of monomeric phospholamban in lipid membranes determined by a hybrid solution and solid-state NMR approach. Proc Natl Acad Sci USA 106:10165–10170

Traaseth NJ, Gopinath T, Veglia G (2010) On the performance of spin diffusion NMR techniques in oriented solids: prospects for resonance assignments and distance measurements from separated local field experiments. J Phys Chem B 114:13872–13880

Tupling AR, Asahi M, MacLennan DH (2002) Sarcolipin overexpression in rat slow twitch muscle inhibits sarcoplasmic reticulum $Ca^{2+}$ uptake and impairs contractile function. J Biol Chem 277:44740–44746

Valentine KG, Liu SF, Marassi FM, Veglia G, Opella SJ, Ding FX, Wang SH, Arshava B, Becker JM, Naider F (2001) Structure and topology of a peptide segment of the 6th transmembrane domain of the saccharomyces cerevisae alpha-factor receptor in phospholipid bilayers. Biopolymers 59:243–256

Veglia G, Ha KN, Shi L, Verardi R, Traaseth NJ (2010) What can we learn from a small regulatory membrane protein? Methods Mol Biol 654:303–319

Verardi R, Shi L, Traaseth NJ, Walsh N, Veglia G (2011) Structural topology of phospholamban pentamer in lipid bilayers by a hybrid solution and solid-state NMR method. Proc Natl Acad Sci USA 108:9101–9106

Vinogradov E, Madhu PK, Vega S (1999) High-resolution proton solid-state NMR spectroscopy by phase-modulated Lee–Goldburg experiment. Chem Phys Lett 314:443–450

Wang J, Denny J, Tian C, Kim S, Mo Y, Kovacs F, Song Z, Nishimura K, Gan Z, Fu R, Quine JR, Cross TA (2000) Imaging membrane protein helical wheels. J Magn Reson 144:162–167

White SH (2009) Biophysical dissection of membrane proteins. Nature 459:344–346

Wu CH, Ramamoorthy A, Opella SJ (1994) High-resolution heteronuclear dipolar solid-state NMR spectroscopy. J Mag Res Series A 109:270–272

Xu J, Struppe J, Ramamoorthy A (2008) Two-dimensional homonuclear chemical shift correlation established by the cross-relaxation driven spin diffusion in solids. J Chem Phys 128:052308

Xu J, Smith PE, Soong R, Ramamoorthy A (2011) A proton spin diffusion based solid-state NMR approach for structural studies on aligned samples. J Phys Chem B 115:4863–4871

Yamamoto K, Dvinskikh SV, Ramamoorthy A (2006) Measurement of heteronuclear dipolar couplings using a rotating frame solid-state NMR experiment. Chem Phys Lett 419:533–536